Catalysis Today 150 (2010) 171–178

Contents lists available at ScienceDirect

Catalysis Today

journal homepage: www.elsevier.com/locate/cattod

Development of new NiMo/γ-alumina catalysts doped with noble metals for deep HDS

Tatiana Klimova *, Paola Mendoza Vara, Ivan Puente Lee

Facultad de Química, Departamento de Ingeniería Química, Universidad Nacional Autónoma de México (UNAM), Cd. Universitaria, Coyoacán, México D.F. (04510), Mexico

ARTICLE INFO

Article history:
Available online 4 September 2009

Keywords:
Deep hydrodesulfurization
4,6-Dimethyldibenzothiophene
NiMo catalysts
Platinum
Palladium
Ruthenium

ABSTRACT

In the present work, with the aim of searching for new, highly effective catalysts for deep HDS, conventional NiMo/γ-Al_2O_3 catalysts were modified by the incorporation of small amounts (1 wt.%) of noble metals (NM = Pt, Pd, Ru) in order to increase their hydrogenation ability. Prepared catalysts were characterized in oxide state by N_2 physisorption, XRD, UV–vis DRS, temperature-programmed reduction and SEM-EDX, and in sulfided state by HRTEM. The catalysts were tested in the 4,6-dimethyldibenzothiophene (4,6-DMDBT) hydrodesulfurization. Results from the catalytic activity tests showed that the nature of the noble metal influences the catalytic performance of trimetallic NMNiMo catalysts supported on alumina. In general, doping of the conventional NiMo/γ-Al_2O_3 catalyst by all noble metals used resulted in an enhancement of the HYD route of 4,6-DMDBT hydrodesulfurization, especially in the case of the Ru-modified sample. However, if Pt and Pd-containing ternary catalysts showed activity 10–20% higher than the reference conventional NiMo/γ-Al_2O_3 sample, Ru addition had a negative effect on the overall catalytic activity. The activity of PdNiMo and PtNiMo/γ-Al_2O_3 catalytic formulations seems to be close to the sum of the activities obtained over NM/γ-Al_2O_3 and NiMo/γ-Al_2O_3 counterparts. This means that there is no synergetic effect between noble metals and conventional NiMo/alumina catalysts.

1. Introduction

A growing interest in the development of novel high performance hydrodesulfurization (HDS) catalysts is explained by the need to produce clean engine fuels by processing poor-quality petroleum feedstocks. Recently, more stringent fuel specifications have been implemented in many countries (European Community, United States and Japan) in order to minimize air pollution and prevent the poisoning of exhaust treatment catalysts [1]. However, the problem of how to reduce the contents of sulfur in petroleum-derived transportation fuels to a very low level (less then 15 ppm of S) is still a major problem to be solved [2–4].

Nowadays, many efforts are aimed to develop new HDS catalysts or to improve the conventional CoMo and NiMo/γ-Al_2O_3 formulations making them able to reach the required levels of sulfur elimination. It is well known that the key for reaching deep HDS of diesel fuel is the elimination of the most refractory polyaromatic sulfur compounds such as dibenzothiophenes (DBT) with alkyl groups in positions 4 and 6 [5–7]. These molecules cannot be transformed into the corresponding desulfurized products via the direct desulfurization route (DDS) because the alkyl groups adjacent to the sulfur atom hinder the σ bonding perpendicular to the catalyst surface required for the C–S bond hydrogenolysis. So, the HDS of refractory DBT compounds occurs predominantly through the hydrogenation (HYD) pathway, in which the reactant molecule is first hydrogenated to intermediates and then the C–S bond is broken and the sulfur atom is removed. Therefore, the hydrogenating functionality of the catalyst is of great importance and determines its activity for deep HDS [8]. Conventional CoMo and NiMo sulfides perform hydrodesulfurization via DDS, which makes them ineffective for deep HDS [9]. On the other hand, the well-known outstanding hydrogenating capacity of noble metals makes them potential catalysts for deep HDS and hydrodearomatization (HDA). Because of this, recently, noble metal catalysts (either supported or unsupported) have received considerable attention, and some attempts have been made to use them in catalytic formulations designed for deep HDS. Unsupported noble metal catalysts (PtS, PdS, RuS_2, etc.) were reported a long time ago as effective catalysts for the HDS of dibenzothiophene at high pressures, more active than MoS_2 [10,11]. The reduced Pt catalysts supported on γ-Al_2O_3, SBA-15 and HZSM-5 were tested by Prins et al. in 4,6-dimethyldibenzothiophene (4,6-DMDBT) hydrodesulfurization [12]. It was observed that Pt catalysts supported on alumina and SBA-15 hydrogenated 4,6-DMDBT fast to the intermediate hexahydro-4,6-DMDBT and removed sulfur from 4,6-DMDBT somewhat slower, giving 3,3′-dimethylbiphenyl. The conversion of 4,6-DMDBT over Pt/HZSM-5 was low, probably because of the solvent hydrocracking and coking of the catalyst. The activities and selectivities of Pt, Pd and Pt-Pd

* Corresponding author. Tel.: +52 55 56225371; fax: +52 55 56225371.
E-mail address: klimova@servidor.unam.mx (T. Klimova).

0920-5861/$ – see front matter © 2009 Elsevier B.V. All rights reserved.
doi:10.1016/j.cattod.2009.08.003

supported on alumina and amorphous silica-alumina were investigated in 4,6-DMDBT HDS by Niquille-Röthlisberger and Prins [8,13,14]. The silica-alumina-supported catalysts had higher activities than alumina-supported analogs. Pd showed a high hydrogenation activity for 4,6-DMDBT, but the removal of sulfur from 4,6-DMDBT and its HDS intermediates occurred faster over Pt than over Pd. Larger metal particles led to relatively faster hydrogenation and slower C-S breaking. A Pt/γ-Al_2O_3 catalyst was tested in simultaneous HDS of DBT and HDA of naphthalene by Centeno and co-workers studying the effect of the sample pretreatment (reduction, sulfidation with H_2S/H_2 mixture or pure H_2S and non-activation) [15]. The reduced catalyst presented the best performance, whereas presulfidation with H_2S/H_2 mixture leading to a mixture of PtS and Pt^0 had a negative effect on the catalytic activity. All the catalysts were selective to the HDS reaction over HDA, and to the direct desulfurization pathway of DBT HDS. Similar studies realized with Pd/γ-Al_2O_3 [16] and Rh/γ-Al_2O_3 [17] catalysts revealed the high selectivity of the former to the HYD route of DBT hydrodesulfurization. In both cases activation with H_2S decreased HYD selectivity. Ishihara et al. systematically monitored the HDS activity of DBT and substituted DBTs present in a SR-LGO over various noble metal catalysts (Ru, Rh, Ru-Rh, Pt, Pd and Pt-Pd) supported on alumina making a comparison with a conventional CoMo catalyst [18]. The Pd-based catalysts exhibited excellent HDS performances, especially for desulfurizing the refractory compounds, which was attributed to the exceptional hydrogenation properties of the Pd-based catalysts. The authors also pointed out that HDS catalysts derived from Rh complexes are promising, especially the ones supported on silica or silica-alumina as a carrier [19]. The HDS behavior of RuS_2 catalysts supported on alumina was also found to depend strongly on the sulfidation procedure, composition of the sulfiding stream, and sulfidation temperature [20,21 and references therein].

Bimetallic noble metal containing catalysts have also attracted considerable attention. Among them, the Pt-Pd system was widely studied by Ishihara et al. [18], Niquille-Röthlisberger and Prins [8,13,14], Yoshimura et al. [22] and Zotin and co-workers [23]. It was found that the combination of Pt and Pd greatly enhanced the HDS activity (the synergetic effect) and the hydrogenation properties of the alumina- and silica-alumina-supported catalysts [8,14]. In addition, these catalysts are less sensitive to inhibition by nitrogen-containing molecules (pyridine and piperidine) [13]. The above behavior was considered the indication that the metal particles were alloyed [8]. Other bimetallic catalyst formulations extensively studied in the last few years are sulfided Mo catalysts doped with noble metals (Pt, Pd, Ru) [24–29]. In general, these binary catalysts showed larger activity than monometallic ones [25]. In all the above-mentioned works, a synergetic effect was detected for noble metal molybdenum catalysts (NM-Mo) in HDS and HYD reactions. However, the magnitude of this effect depended on the kind of noble metal used, NM/(NM + Mo) atomic ratio and reaction type (HDS or HYD). In some cases, Pt-Mo catalysts showed stronger synergetic effect than Ru-Mo ones [24], but in other cases the opposite tendency was observed [26]. However, in general the activity of NM-Mo binary formulations was smaller or comparable to that of the traditional NiMo or CoMo catalysts [24,25].

In order to achieve ultra-deep desulfurization of diesel fuel, recently, commercial Ni(Co)Mo/γ-Al_2O_3 catalysts were improved by the addition of small amounts of noble metals [30,31]. Thus, Geantet and co-workers [30] examined a catalytic system based on the addition of a low content of Pt to commercial NiMo, CoMo, or NiW on alumina catalysts. Catalytic activity of these formulations was tested in the hydrogenation of tetraline, the hydrodesulfurization of DBT, and the straight run gas oil conversion. It was found that a 20–40% increase in the activity can be reached if Pt is impregnated on a presulfided commercial HDT catalyst. In all cases, Pt addition resulted in an improvement in the catalytic hydrogenation activity. On the contrary, when Pt was impregnated on the oxidic form of the catalyst a sharp decrease in the activity was observed. This behavior was ascribed to detrimental interactions between Pt and "NiWS" or "CoMoS" phases. Navarro et al. also modified commercial Ni(Co)Mo/γ-alumina catalysts by the addition of Pd and Ru in order to enhance their hydrogenation function as required for the simultaneous elimination of sulfur, nitrogen and aromatics from a gasoil [31]. The catalysts were prepared by wet impregnation of the commercial samples with Ru and Pd salt solutions and tested in the HDS of DBT and in the hydrotreating of straight run gas oil. Catalyst screening in the HDS of DBT showed that catalyst doping with Ru was more effective than its doping with Pd and that the NiMo catalyst formulation was more effective than its CoMo counterpart.

In the present work, we continue inquiring into the possibility of increasing the HYD ability of the conventional NiMo/γ-Al_2O_3 catalyst by the incorporation of small amounts of different noble metals (NM) in order to make it more appropriate for deep HDS. For this aim, a series of NMNiMo/γ-Al_2O_3 formulations (NM = Pt, Pd, Ru) were prepared, characterized and tested in 4,6-dimethyldibenzothiophene HDS reaction. The principal objective of this study was to clarify the effect of noble metal nature on the behavior (activity as well as selectivity) of noble metal-nickel-molybdenum trimetallic catalysts supported on γ-Al_2O_3 in the elimination of strongly hindered sulfur compounds.

2. Experimental

2.1. Support and catalyst preparation

Alumina support (γ-Al_2O_3) was synthesized by calcination of Boehmite Catapal B at 700 °C for 4 h. After calcination the γ-Al_2O_3 support was sieved to 0.15–0.25 mm size. NiMo catalysts supported on γ-alumina were prepared by successive incipient wetness impregnation (Mo first) with aqueous solutions of ammonium heptamolybdate, $(NH_4)_6Mo_7O_{24}{\cdot}4H_2O$ (Aldrich), and nickel nitrate, $Ni(NO_3)_2{\cdot}6H_2O$ (Aldrich). After each impregnation, the catalysts were dried (2 h at ambient temperature and then 24 h at 100 °C) and calcined (500 °C, 4 h, heating ramp 3 °C min^{-1}). Noble metals were added to the NiMo/γ-Al_2O_3 sample by incipient wetness impregnation of solutions of corresponding NM precursors. Palladium(II) acetate, $Pd(OAc)_2$, (98%, Aldrich), chloroplatinic(IV) acid hydrate, $H_2PtCl_6{\cdot}xH_2O$ (99.9%, Aldrich), and ruthenium(III) acetylacetonate, $Ru(acac)_3$ (97%, Aldrich) were used as NM precursors without further purification. NM impregnation was realized using solutions of Pd salt in acetone, chloroplatinic acid in water and Ru complex in ethanol. NM-containing catalysts were dried and calcined as described above. The nominal metal loadings in the catalysts were 12 wt.% of MoO_3, 3 wt.% of NiO and 1 wt.% of NM. The prepared catalysts will be denoted as NiMo/γ-Al_2O_3 and NMNiMo/γ-Al_2O_3, respectively.

2.2. Support and catalyst characterization

The support and catalysts were characterized by N_2 physisorption, X-ray diffraction (XRD), UV–vis diffuse reflectance spectroscopy (DRS), temperature-programmed reduction (TPR), SEM-EDX and HRTEM. N_2 adsorption/desorption isotherms were measured with a Micromeritics ASAP 2000 automatic analyzer at liquid N_2 temperature. Prior to the experiments, the samples were degassed ($p < 10^{-1}$ Pa) at 270 °C for 6 h. Specific surface areas were calculated by the BET method (S_{BET}), the total pore volume (V_p) was determined by nitrogen adsorption at a relative pressure of 0.98 and pore size distributions from both the adsorption and the desorption isotherms by the BJH method. The mesopore diameters

Table 1
Textural characteristics and chemical composition of NMNiMo/γ-Al_2O_3 catalysts.

Sample	Chemical composition (wt.%)[a]			S_{BET} (m^2/g)	V_P (cm^3/g)	D_{ads}[b] (Å)	D_{des}[c] (Å)
	MoO_3	NiO	NM				
γ-Al_2O_3	–	–	–	200	0.48	110	75
Pt/γ-Al_2O_3	–	–	1.14	199	0.47	110	78
Pd/γ-Al_2O_3	–	–	1.00	188	0.47	110	76
Ru/γ-Al_2O_3	–	–	0.95	176	0.44	110	75
NiMo/γ-Al_2O_3	12.35	3.08	–	185	0.39	110	73
PtNiMo/γ-Al_2O_3	12.49	3.15	0.97	172	0.39	110	75
PdNiMo/γ-Al_2O_3	12.46	3.09	1.09	175	0.40	110	75
RuNiMo/γ-Al_2O_3	11.95	2.93	1.02	182	0.40	110	73

[a] As determined by SEM-EDX.
[b] Pore diameter determined from the adsorption isotherm by the BJH method.
[c] Pore diameter determined from the desorption isotherm by the BJH method.

(D_{ads} and D_{des}) correspond to the maxima of the pore size distributions obtained from adsorption and desorption isotherms, respectively. Powder XRD patterns were recorded in the $3^\circ \leq 2\Theta \leq 90^\circ$ range on a Siemens D5000 diffractometer, using Cu Kα radiation (λ = 1.5406 Å) and a goniometer speed of $1^\circ(2\Theta)$ min^{-1}. UV–vis–NIR electronic spectra of the samples were recorded in the wavelength range 200–800 nm using a Varian Cary 100 spectrophotometer equipped with a diffuse reflectance attachment. Polytetrafluoroethylene was used as reference. TPR experiments were carried out in a Micromeritics AutoChem II 2920 automatic analyzer equipped with a TC detector. In the TPR experiments, the samples were pretreated *in situ* at 500 °C for 2 h under air flow and cooled in an Ar stream. The reduction step was performed with an Ar/H_2 mixture (90/10 mol/mol, 50 ml/min), with a heating rate of 10 °C/min, up to 1000 °C. Chemical composition of catalysts was determined by SEM-EDX using JEOL 5900 LV microscope with OXFORD ISIS equipment. High resolution transmission electron microscopy (HRTEM) images and selected area electron diffraction (SAED) patterns were recorded with JEOL 2010 microscope (resolving power 1.9 Å at 200 kV). The solids were ultrasonically dispersed in heptane and the suspension was collected on carbon coated grids. HRTEM pictures were taken from different parts of the same sample dispersed on the microscope grid. Average slab length and layer number of MoS_2 crystallites (Table 2) were established from the measurement of at least 300 crystallites detected on several HRTEM pictures of each sample.

2.3. Catalytic activity

The 4,6-DMDBT HDS activity tests were performed in a batch reactor at 300 °C and 7.3 MPa total pressure for 8 h. Prior to the catalytic activity evaluation, the catalysts (0.15 g) were sulfided *ex situ* in a tubular reactor at 400 °C for 4 h in a stream of 15 vol.% of H_2S in H_2 under atmospheric pressure. After cooling down to room temperature under the same sulfiding mixture and flushing with nitrogen for 30 min, the catalysts were transferred under argon to the batch reactor containing 40 ml of 4,6-DMDBT solution in hexadecane (0.024 mol/l, 1000 ppm S). The course of the reaction was followed by withdrawing aliquots each hour and analyzing them on an HP-6890 chromatograph. To corroborate product identification, the product mixture was analyzed on a Hewlett Packard GC-MS instrument.

3. Results and discussion

3.1. Characterization of catalysts in their oxide state

Chemical analysis results (Table 1) show that the actual chemical compositions (Ni, Mo and NM loading) of the prepared catalysts are close to the expected nominal ones, 12 wt.% MoO_3, 3 wt.% NiO and ~1 wt.% NM. The results from textural characterization of γ-Al_2O_3 support and corresponding NiMo and NMNiMo catalysts are also shown in Table 1. It can be observed that BET surface area and total pore volume slightly decreased after metal incorporation. However, this decrease was proportional to the metal loading in the catalysts. Pore diameter determined from the adsorption and desorption branches of the isotherm was almost not affected by the metal incorporation. In line with this, the shape of the nitrogen adsorption–desorption isotherm characteristic of γ-alumina (type IV isotherm with the hysteresis loop belongs to type H2) was not changed after Ni, Mo and NM addition (Fig. 1). XRD patterns of NiMo and NMNiMo/γ-Al_2O_3 catalysts did not show the presence of any crystalline phase with the exception of γ-Al_2O_3 from the support. The above results point out good dispersion of Mo, Ni and NM species in the catalysts in their oxide form. UV–vis DRS spectra (not shown) of NiMo/γ-Al_2O_3 and NMNiMo/γ-Al_2O_3 catalysts were very similar to those reported previously in literature for alumina-supported NiMo catalysts [32,33]. In all cases, a presence of a complex mixture of Mo^{6+} species in tetrahedral and octahedral coordination was observed. No changes in the proportion of different types of Mo species or in the position of the absorption edge were detected in the DRS spectra of the catalysts after NM incorporation.

Results from TPR characterization of the prepared oxidic NiMo and NMNiMo catalysts are shown in Fig. 2. For NiMo/γ-Al_2O_3, three peaks can be observed (curve (a), Fig. 2). The assignation of the TPR hydrogen consumption peaks has been made on the basis of the previous literature reports on Mo and NiMo catalysts supported on alumina [34,35]. The low-temperature peak (maximum at 372 °C) can be assigned to the first step of reduction of Mo^{6+} to Mo^{4+} in

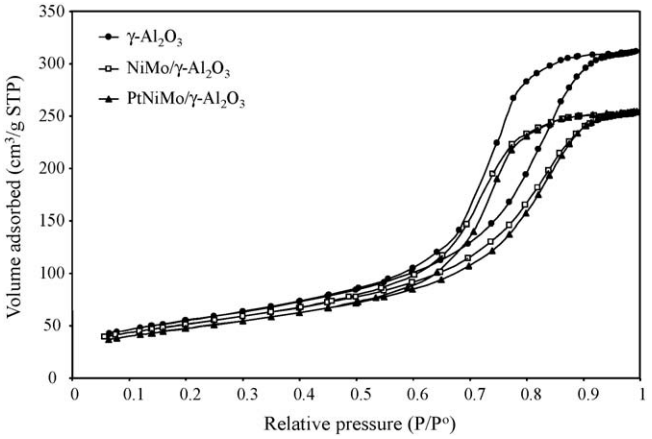

Fig. 1. Nitrogen adsorption–desorption isotherms of γ-Al_2O_3 support and corresponding NiMo and PtNiMo catalysts.

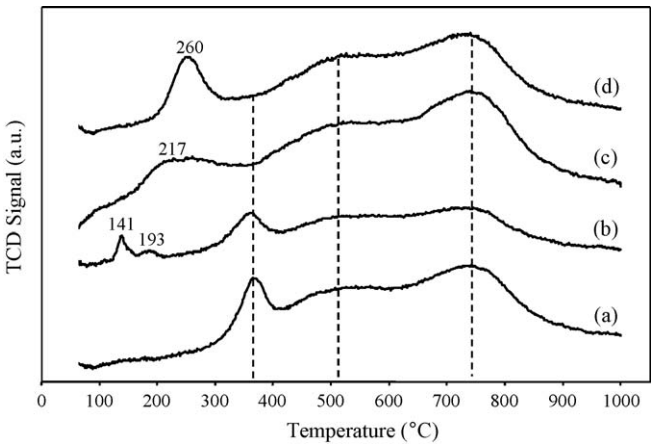

Fig. 2. TPR profiles for the reference NiMo/γ-Al_2O_3 catalyst (a) and noble metal doped formulations: RuNiMo/γ-Al_2O_3 (b); PdNiMo/γ-Al_2O_3 (c); and PtNiMo/γ-Al_2O_3 (d). The curves are shifted for clarity and correspond to the same catalyst weight.

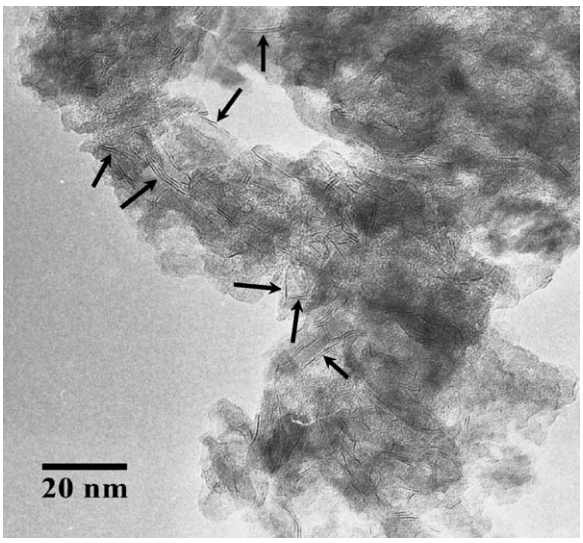

Fig. 3. HRTEM micrograph of sulfided NiMo/γ-Al_2O_3 catalyst.

dispersed polymeric Mo structures (octahedral Mo species), whereas hydrogen consumption in the temperature range between 450 and 650 °C can be ascribed to the similar step of reduction of octahedral Mo species of higher degree of polymerization up to orthorhombic MoO_3, which reduces around 600–630 °C. In the high-temperature region, a large peak with the maximum at 745 °C can be observed. This peak is generally associated with a further progress in the reduction of Mo^{4+} species obtained at lower temperatures, as well as with the reduction of tetrahedral Mo^{6+} species strongly interacting with the alumina support. The TPR profiles of the NiMo/γ-Al_2O_3 catalysts modified by the incorporation of noble metals are also shown in Fig. 2, curves (b)–(d). The profile of the RuNiMo/γ-Al_2O_3 sample is similar to the described above for the starting NiMo/γ-Al_2O_3 reference, with the exception of two new signals observed in the range 120–220 °C. These two peaks can be ascribed to the reduction of Ru species supported on alumina, namely the first peak at 141 °C corresponds to the reduction of a well-dispersed ruthenium phase and the second (at 193 °C) to the reduction of RuO_2 species [25,36]. Similarly, the TPR profiles of Pt- and Pd-containing trimetallic catalysts (curves (c) and (d), Fig. 2) show hydrogen consumption at low temperatures (below 300 °C), which can be related to the reduction of the corresponding Pt or Pd species [37]. However, these two TPR patterns have distinctive features, which are the absence of a peak with the maximum at 372 °C observed in the TPR profile of the starting NiMo/γ-Al_2O_3 catalyst attributed to the reduction of dispersed octahedral Mo^{6+} species and an increase in hydrogen consumption at temperatures below 300 °C. The latter is much higher than the amount which can be attributed to the reduction of the corresponding NM species, indicating that some of the Mo^{6+} species are also reduced in the low-temperature region. It seems that the reduction of the most easily reduced Mo phase became even easier after Pt (Pd) incorporation in the NiMo/γ-Al_2O_3 sample. Different explanations can be proposed for the above observation. On the one hand, it can be supposed that octahedral Mo^{6+} species were re-dispersed along with the impregnation of noble metal precursors. This supposition is in line with previous observations by López Cordero and López Agudo, who found that these Mo species can be easily extracted with water [34], and by Fierro et al. who observed the re-dispersion of MoO_3 crystals during the second step of preparation of bimetallic NM-Mo catalysts, namely, the step of impregnation of NM [25]. On the other hand, it is possible that Pt (Pd) could facilitate reduction of the octahedral Mo species of the NMNiMo formulations. Similar behavior during TPR was observed recently for Pt modified MoS_2/silica-alumina and explained by easier reduction of the MoS_2 phase in presence of Pt [29]. Regarding the peaks observed in the TPR profiles of all NMNiMo/γ-Al_2O_3 samples at temperatures above 450 °C, no differences were observed with respect to the starting NiMo/γ-Al_2O_3 material, indicating that NM incorporation in the conventional NiMo catalyst supported on alumina did not produce significant changes in the characteristics of Mo species reducible in the high-temperature range (450–1000 °C). Resuming the above results, it can be concluded that the incorporation of the noble metals used in this work (Pd, Pt, Ru) in the conventional NiMo/γ-Al_2O_3 catalyst did not produce significant changes in the characteristics of oxide NiMo species. Only some increase in the ease of reduction of octahedral Mo species was observed for the Pt- and Pd-containing formulations.

3.2. Characterization of sulfided catalysts

HRTEM characterization of the sulfided catalysts was undertaken in order to characterize the morphology of both MoS_2 phase and NM particles. The obtained micrographs are shown in Figs. 3–6. The typical fringes due to MoS_2 crystallites with 6.1 Å interplanar distances were observed on micrographs of all sulfided catalysts. Fig. 3 shows a representative HRTEM micrograph of sulfided NiMo/γ-Al_2O_3 catalyst. The slabs are homogeneously distributed over the alumina surface. The length of the MoS_2 crystallites in this catalyst was between 20 and 80 Å. The average slab length was calculated to be 45 Å (Table 2). The number of stacking layers was between 1 and 3, with an average of 1.8 layers. It can be seen in Figs. 4, 6 and 7 and Table 2 that in the catalysts modified by NM loading, MoS_2 particles have similar features. Therefore, the addition of noble metals in the conventional NiMo catalyst supported on alumina almost did not affect the morphology of MoS_2 particles.

Regarding the noble metal particles, their morphology can also been observed in the micrographs of sulfided NMNiMo/γ-Al_2O_3 samples. Thus, among the three NM-containing samples, Pt particles were seen better (Fig. 4). Their shape and size were not regular, as it can be seen in Fig. 4(b). Pt particles with the size between 30 and 200 Å were observed, some of which do not have a regular shape, whereas others do, as it is shown in Fig. 4(c). In the SAED pattern of the sulfided PtNiMo/γ-Al_2O_3 catalyst, diffraction spots from both metallic Pt and sulfided PtS phase, known as cooperite, were present in addition to the continuous rings of γ-

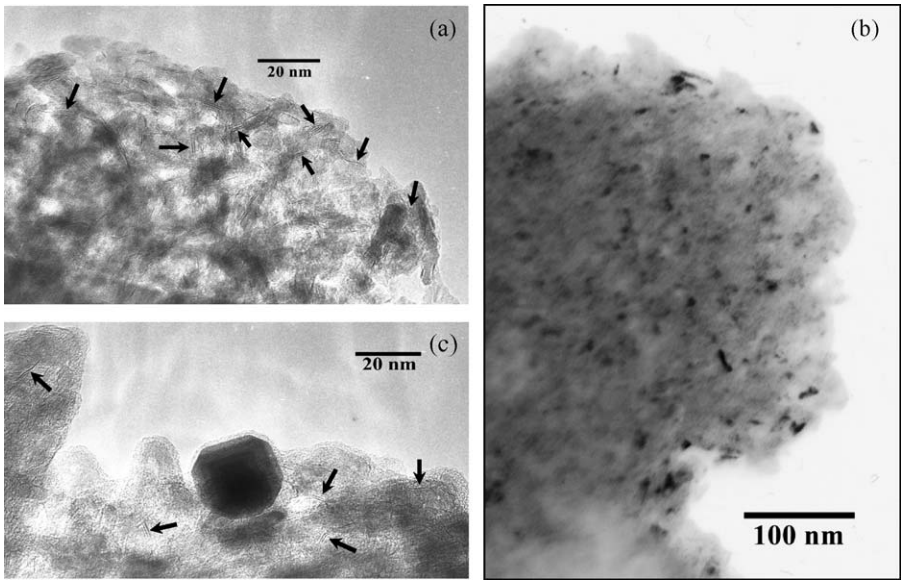

Fig. 4. HRTEM micrographs of sulfided PtNiMo/γ-Al_2O_3 catalyst.

Al_2O_3 (Fig. 5). So it can be concluded that PtS and Pt^0 phases coexist in the PtNiMo/γ-Al_2O_3 catalyst sulfided in H_2S/H_2 stream. This result is well in line with a previous report [15] for Pt/γ-Al_2O_3 samples sulfided in similar conditions. Pd and Ru particles can also be seen in Figs. 6 and 7 (although not as clear as Pt particles in Fig. 4). In general it can be observed that the shape of NM particles was spherical or quasi-spherical and they were distributed homogeneously over the alumina surface.

3.3. Catalytic activity

The catalytic activity of sulfided NiMo/γ-Al_2O_3 catalysts doped with Pt, Pd and Ru was examined in the hydrodesulfurization of 4,6-dimethyldibenzothiophene. The conversions of 4,6-DMDBT obtained over different catalysts at various reaction times are shown in Table 3. Results obtained with corresponding monometallic NM/γ-Al_2O_3 samples and with the conventional NiMo/γ-Al_2O_3 catalyst are also included in Table 3 for comparison purposes. As it can be seen, monometallic Pt, Pd and Ru catalysts supported on alumina showed low activity in 4,6-DMDBT hydrodesulfurization, especially the Ru one. The order of activity for the monometallic catalysts is Pd > Pt ≫ Ru. Regarding the activity of trimetallic PtNiMo, PdNiMo and RuNiMo/γ-Al_2O_3 catalysts, all resulted to be significantly more active than the corresponding monometallic NM/γ-Al_2O_3 counterparts. Platinum and palladium containing ternary formulations were found to be 10–20% more active than the reference NiMo/γ-Al_2O_3 sample, whereas the ruthenium addition in the conventional catalyst had a detrimental effect on its HDS activity. The order of NM-containing NiMo formulations according to their activity in 4,6-DMDBT hydrodesulfurization is PtNiMo/γ-Al_2O_3 > PdNiMoγ-Al_2O_3 > reference NiMo/γ-Al_2O_3 > RuNiMo/γ-Al_2O_3. The activity of PdNiMo and PtNiMo/γ-Al_2O_3 catalytic formulations seems to be close to the sum of the activities obtained over corresponding monometallic Pt or Pd catalysts supported on γ-Al_2O_3 and the conventional NiMo/γ-Al_2O_3 counterpart (Table 3).

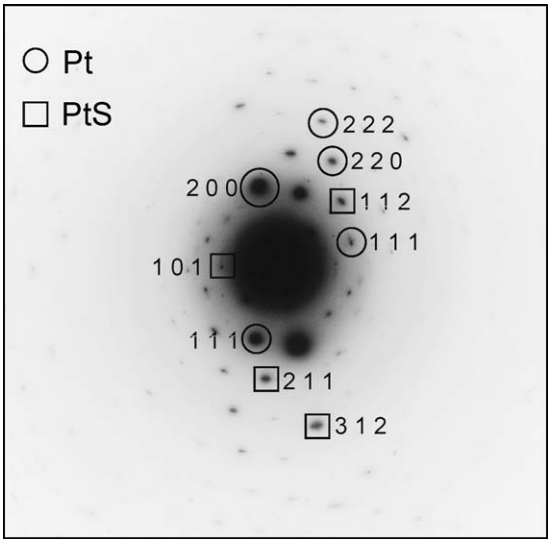

Fig. 5. SAED pattern of sulfided PtNiMo/γ-Al_2O_3 catalyst.

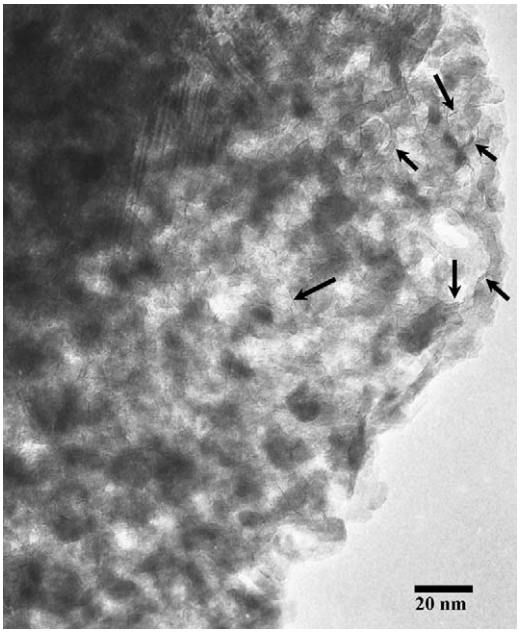

Fig. 6. HRTEM micrograph of sulfided PdNiMo/γ-Al_2O_3 catalyst.

Table 2
Average length and layer number of the MoS_2 crystallites determined by HRTEM.

Catalyst	Average length (Å)	Average stacking
NiMo/γ-Al_2O_3	45	1.8
PtNiMo/γ-Al_2O_3	44	1.7
PdNiMo/γ-Al_2O_3	46	1.7
RuNiMo/γ-Al_2O_3	45	1.8

This means that there is no synergetic effect between noble metals and conventional NiMo/alumina catalysts. A similar result was observed previously by Geantet and co-workers [30] in the study of the hydrogenation activity of conventional industrial NiMo, NiW and CoMo on alumina catalysts doped with a small amount of Pt. When Pt was added after the sulfidation of the commercial catalyst, the catalytic properties of these Pt-doped formulations in tetraline conversion seemed to correspond to the addition of the properties of each component. In our case, we observed the same effect although the noble metal dopants were added in the catalyst in its oxidic form prior to sulfidation. The results from the HRTEM characterization described above for the sulfided catalysts prepared in this work seem to be in agreement with the catalytic behavior of trimetallic catalysts. Thus, noble metal and MoS_2 phases were observed to exist separately on the alumina surface, being the morphology of the MoS_2 crystallites almost the same as in the starting conventional NiMo/γ-Al_2O_3.

Among all catalysts tested, the ruthenium-containing ones (Ru/γ-Al_2O_3 and RuNiMo/γ-Al_2O_3) showed the lowest activity in 4,6-DMDBT HDS. This result is in accordance with a previous report [24] in which monometallic NM/γ-Al_2O_3 catalysts with 0.5 wt.% of NM were sulfided in different conditions and tested in HDS of dibenzothiophene and HYD of naphthalene. Ru/γ-Al_2O_3 catalyst also showed very low activity for both HDS and HYD reactions in disagreement with some other literature reports. This fact was attributed by the authors of [24] to the low content of Ru in the catalysts and to the calcination and sulfidation conditions used. De Los Reyes recently revised available bibliographic information regarding the effect of synthesis methods and activation procedures on the catalytic properties for RuS_2 supported on Al_2O_3 [21]. From literature analysis, he made a conclusion that in order to obtain highly active Ru catalysts, it is necessary to avoid calcination before RuS_2 activation. In the present work, all catalysts (monometallic as well as trimetallic) were treated following the same experimental procedure including calcination in air and sulfidation in a stream of H_2S-H_2 mixture prior to catalytic activity tests. This seems to be the reason for such low activity of Ru-containing samples.

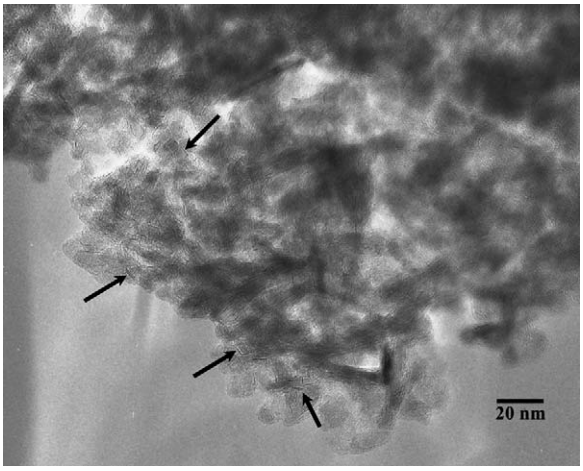

Fig. 7. HRTEM micrograph of sulfided RuNiMo/γ-Al_2O_3 catalyst.

Table 3
Activity of the tested catalysts in 4,6-DMDBT hydrodesulfurization.

Sample	4,6-DMDBT conversion (%)[a]			
	2	4	6	8
Pt/γ-Al_2O_3	1.1	2.4	4.9	11.5
Pd/γ-Al_2O_3	1.8	4.0	7.8	12.9
Ru/γ-Al_2O_3	N.D.[b]	N.D.	N.D.	2.4
NiMo/γ-Al_2O_3	12.6	27.8	40.1	55.8
PtNiMo/γ-Al_2O_3	11.4	32.3	51.7	67.2
PdNiMo/γ-Al_2O_3	11.1	33.3	48.4	62.6
RuNiMo/γ-Al_2O_3	7.0	18.8	31.0	40.6

[a] At different reaction time (h).
[b] N.D.: not determined.

The analysis of the catalysts' selectivity was done on the basis of the well-known scheme of 4,6-DMDBT hydrodesulfurization (Fig. 8). The HDS of 4,6-dimethyldibenzothiophene occurs through two parallel reaction routes. The first one is called the direct desulfurization (DDS) pathway and comprises direct elimination of S atom via C–S bond cleavage yielding the corresponding dimethylbiphenyl (DMBP) product. The second, usually called the HYD pathway, consists in the hydrogenation of one of the benzene rings of 4,6-DMDBT followed by hydrogenolysis. This pathway yields first tetrahydrodimethyldibenzothiophene (THDBT), then the corresponding hexahydro-derivative (HHDBT) and finally, methylcyclohexyltoluene (MCHT). Between the two reaction routes mentioned above, the HYD pathway is the preferred route for the hydrodesulfurization of 4,6-dimethyldibenzothiophene [2,38]. Because of this, small amounts of noble metals were added in the conventional NiMo/γ-Al_2O_3 catalyst in order to improve its catalytic performance and favor the hydrogenation pathway.

The reaction product distributions obtained with NM-containing catalysts are shown in Tables 4 and 5 for two values of the total 4,6-DMDBT conversion (12 and 35%). The ratios between different products involved in the reaction network of 4,6-DMDBT hydrodesulfurization are presented in Table 6. It can be observed in Table 4, in line with previous reports [8,13,14], that monometallic Pd/γ-Al_2O_3 catalyst has excellent hydrogenation ability, but is not

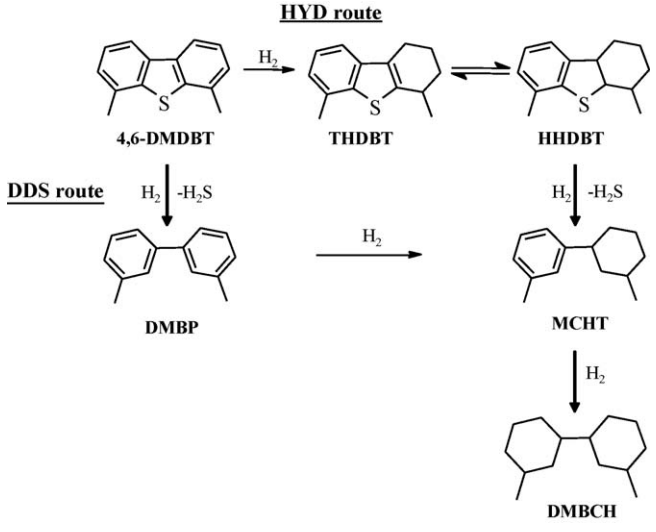

Fig. 8. Reaction network for 4,6-dimetyldibenzothiophene hydrodesulfurization. THDBT, tetrahydrodimethyldibenzothiophene; HHDBT, hexahydrodimethyldibenzothiophene; MCHT, methylcyclohexyltoluene; DMBCH, dimethylbicyclohexyl; DMBP, dimethylbiphenyl.

Table 4
Selectivity of the different catalysts in 4,6-DMDBT HDS at 12% of 4,6-DMDBT conversion.

Catalyst	Product composition (%)[a]					Pre-hydrogenated intermediates (%)[b]	Desulfurized products (%)[c]
	THDBT	HHDBT	DMBP	MCHT	DMBCH		
NiMo/γ-Al_2O_3	27.2	5.4	28.5	35.1	3.8	32.6	67.4
Pt/γ-Al_2O_3	24.6	5.4	20.5	38.5	11.0	30.0	70.0
Pd/γ-Al_2O_3	49.9	19.6	4.9	20.0	5.6	69.5	30.5
PtNiMo/γ-Al_2O_3	24.3	7.1	12.6	46.3	9.7	31.4	68.6
PdNiMo/γ-Al_2O_3	21.0	6.0	12.6	49.5	10.9	27.0	73.0
RuNiMo/γ-Al_2O_3	23.9	7.5	11.5	48.1	9.0	31.4	68.6

[a] THDBT, tetrahydrodimethyldibenzothiophene; HHDBT, hexahydrodimethyldibenzothiophene; DMBP, dimethylbiphenyl; MCHT, methylcyclohexyltoluene; DMBCH, dimethylbicyclohexyl.
[b] Sum of THDBT and HHDBT.
[c] Sum of DMBP, MCHT and DMBCH.

Table 5
Selectivity of the different catalysts in 4,6-DMDBT HDS at 35% of 4,6-DMDBT conversion.

Catalyst	Product composition (%)[a]					Pre-hydrogenated intermediates (%)[b]	Desulfurized products (%)[c]
	THDBT	HHDBT	DMBP	MCHT	DMBCH		
NiMo/γ-Al_2O_3	15.4	5.3	8.0	57.3	14.0	20.7	79.3
PtNiMo/γ-Al_2O_3	15.4	4.8	7.2	57.8	14.8	20.2	79.8
PdNiMo/γ-Al_2O_3	14.1	4.4	6.9	59.7	14.9	18.5	81.5
RuNiMo/γ-Al_2O_3	13.4	4.3	6.5	63.0	12.8	17.7	82.3

[a] THDBT, tetrahydrodimethyldibenzothiophene; HHDBT, hexahydrodimethyldibenzothiophene; DMBP, dimethylbiphenyl; MCHT, methylcyclohexyltoluene; DMBCH, dimethylbicyclohexyl.
[b] Sum of THDBT and HHDBT.
[c] Sum of DMBP, MCHT and DMBCH.

Table 6
Reaction product ratios obtained over tested catalysts at different 4,6-DMDBT conversions.

Catalyst	THDBT + HHDBT[a] DMBP		MCHT DMBP		MCHT + DMBCH DMBP	
	12%[b]	35%	12%	35%	12%	35%
Reference NiMo/γ-Al_2O_3	1.1	2.6	1.2	7.2	1.4	8.9
Pt/γ-Al_2O_3	1.5	–	1.9	–	2.4	–
Pd/γ-Al_2O_3	14.2	–	4.1	–	5.2	–
PtNiMo/γ-Al_2O_3	2.5	2.8	3.7	8.0	4.4	10.1
PdNiMo/γ-Al_2O_3	2.1	2.7	3.9	8.7	4.8	10.8
RuNiMo/γ-Al_2O_3	2.7	3.3	4.2	11.6	5.0	13.9

[a] THDBT, tetrahydrodimethyldibenzothiophene; HHDBT, hexahydrodimethyldibenzothiophene; DMBP, dimethylbiphenyl; MCHT, methylcyclohexyltoluene; DMBCH, dimethylbicyclohexyl.
[b] 4,6-DMDBT conversion.

as good as Pt/γ-Al_2O_3 for sulfur elimination from the pre-hydrogenated intermediates. As expected, the addition of noble metals in the conventional catalyst formulation resulted in all cases in an increase in the proportion of the products obtained via the HYD route. This effect is more appreciable at low 4,6-DMDBT conversion (12%), and becomes less pronounced at higher conversion values (Table 6). This result illustrates the importance of the participation of noble metals in the first step of 4,6-DMDBT transformation leading to the formation of the pre-hydrogenated derivatives, which can be subsequently desulfurized on the active sites of another appropriate phase, either transition metal sulfide (MoS_2) or a noble metal one, as in the case of Pt catalysts. In addition, it should be mentioned that for all studied NM-doped NiMo/γ-Al_2O_3 catalysts reaction product ratios shown in Table 6 were similar. However, it can be noted that the Ru-containing NiMo/γ-Al_2O_3 formulation resulted in slightly higher proportions of products obtained via the HYD route than those from the DDS route in comparison to the product ratios obtained with Pt and Pd-doped catalysts. The hydrogenation ability of noble metals incorporated in the conventional NiMo/γ-Al_2O_3 catalyst changes in the following order: Ru > Pd > Pt, which is opposite to the overall catalytic activity trends (Table 3), indicating by this means that in order to improve the catalytic performance of the catalyst in deep HDS it is necessary to reach an optimum ratio between hydrogenation and hydrogenolysis functionalities of the catalytic system.

4. Conclusions

In the present work, in order to solve the problem of deep HDS of diesel fuel, catalysts with improved hydrogenation ability were prepared by the incorporation of small amounts of noble metals (Pt, Pd, Ru) in the conventional NiMo/γ-Al_2O_3 catalyst. Noble metals were added by incipient wetness impregnation of the conventional NiMo/alumina catalyst in its oxide state with solutions of corresponding NM precursors. Characterization of the prepared catalysts showed that NM incorporation in the NiMo/γ-Al_2O_3 sample almost did not affect its textural characteristics and the dispersion and coordination state of the deposited Ni and Mo species. Only when Pt and Pd were impregnated on the NiMo/γ-Al_2O_3 surface from water and acetone solutions, respectively, some increase in the ease of reduction of octahedral Mo species

took place. In line with this, HRTEM characterization of sulfided trimetallic catalysts showed that the morphology of the MoS_2 phase was similar to that of the conventional NiMo/γ-Al_2O_3, whereas noble metals formed particles separate from MoS_2 slabs. The catalysts' tests in the 4,6-dimethyldibenzothiophene HDS showed that the catalytic performance of trimetallic NMNiMo catalysts supported on alumina depends on the nature of the noble metal. Thus, doping of the conventional NiMo/γ-Al_2O_3 catalyst by all noble metals used resulted in an enhancement of the HYD route of 4,6-DMDBT hydrodesulfurization, especially in the case of the Ru-modified sample. Pt and Pd-containing ternary catalysts showed activity 10–20% higher than the reference conventional NiMo/γ-Al_2O_3 sample, while Ru addition had a negative effect on the catalytic activity. The activity of PdNiMo and PtNiMo/γ-Al_2O_3 catalytic formulations seems to be close to the sum of the activities obtained over NM/γ-Al_2O_3 and NiMo/γ-Al_2O_3 counterparts pointing out the absence of synergetic effect between noble metals and conventional NiMoS active phase.

Acknowledgements

Financial support by DGAPA-UNAM, Mexico (grant IN-110609) is acknowledged. The authors thank C. Salcedo for technical assistance with XRD characterizations.

References

[1] U.S. Environmental Protection Agency, http://www.epa.gov/otaq/highway-diesel/index.htm, http://www.epa.gov/otaq/gasoline.htm, 2006.
[2] C. Song, X. Ma, Appl. Catal. B: Environ. 41 (2003) 207.
[3] K.-H. Choi, N. Kunisada, Y. Korai, I. Mochida, K. Nakano, Catal. Today 86 (2003) 277.
[4] S.K. Bej, S.K. Maity, U.T. Turaga, Energy Fuels 18 (2004) 1227.
[5] C. Song, Catal. Today 86 (2003) 211.
[6] L. Vradman, M.V. Landau, M. Herskowitz, Catal. Today 48 (1999) 41.
[7] K.G. Knudsen, B.H. Cooper, H. Topsøe, Appl. Catal. A: Gen. 189 (1999) 205.
[8] A. Niquille-Röthlisberger, R. Prins, Catal. Today 123 (2007) 198.
[9] F. Bataille, J.-L. Lemberton, P. Michaud, G. Pérot, M. Vrinat, M. Lemaire, E. Schulz, M. Breysse, S. Kasztelan, J. Catal. 191 (2000) 409.
[10] T.A. Pecoraro, R.R. Chianelli, J. Catal. 67 (1981) 430.
[11] R.R. Chianelli, T.A. Pecoraro, T.R. Halbert, W.-H. Pan, E.I. Stiefel, J. Catal. 86 (1984) 226.
[12] H. Guo, Y. Sun, R. Prins, Catal. Today 130 (2008) 249.
[13] A. Niquille-Röthlisberger, R. Prins, Ind. Eng. Chem. Res. 46 (2007) 4124.
[14] A. Niquille-Röthlisberger, R. Prins, J. Catal. 242 (2006) 207.
[15] V.G. Baldovino-Medrano, S.A. Giraldo, A. Centeno, Fuel 87 (2008) 1917.
[16] V.G. Baldovino-Medrano, S.A. Giraldo, A. Centeno, J. Mol. Catal. A: Chem. 301 (2009) 127.
[17] S.A. Giraldo, M.H. Pinzón, A. Centeno, Catal. Today 133–135 (2008) 239.
[18] A. Ishihara, F. Dumeignil, J. Lee, K. Mitsuhashi, E.W. Qian, T. Kabe, Appl. Catal. A: Gen. 289 (2005) 163.
[19] J. Lee, A. Ishihara, F. Dumeignil, E.W. Qian, T. Kabe, J. Mol. Catal. A: Chem. 213 (2004) 207.
[20] P. Castillo-Villalón, J. Ramírez, F. Maugé, J. Catal. 260 (2008) 65.
[21] J.A. De Los Reyes, Appl. Catal. A: Gen. 322 (2007) 106.
[22] Y. Yoshimura, M. Toba, H. Farag, K. Sakanishi, Catal. Surv. From Asia 8 (2004) 47.
[23] E. Devers, C. Geantet, P. Afanasiev, M. Vrinat, M. Aouine, J.L. Zotin, Appl. Catal. A: Gen. 322 (2007) 172.
[24] L.I. Merino, A. Centeno, S.A. Giraldo, Appl. Catal. A: Gen. 197 (2000) 61.
[25] B. Pawelec, R.M. Navarro, J.M. Campos-Martin, A. López Agudo, P.T. Vasudevan, J.L.G. Fierro, Catal. Today 86 (2003) 73.
[26] Z. Vít, D. Gulková, L. Kaluža, M. Zdražil, J. Catal. 232 (2005) 447.
[27] D. Pérez-Martínez, S.A. Giraldo, A. Centeno, Appl. Catal. A: Gen. 315 (2006) 35.
[28] M.H. Pinzón, A. Centeno, S.A. Giraldo, Appl. Catal. A: Gen. 302 (2006) 118.
[29] D. Gulková, Y. Yoshimura, Z. Vít, Appl. Catal. B: Environ. 87 (2009) 171.
[30] S. Pessayre, C. Geantet, R. Bacaud, M. Vrinat, T.S. N'Guyen, Y. Soldo, J.L. Hazemann, M. Breysse, Ind. Eng. Chem. Res. 46 (2007) 3877.
[31] R.M. Navarro, P. Castaño, M.C. Alvarez-Galván, B. Pawelec, Catal. Today 143 (2009) 108.
[32] C.C. Williams, J.G. Ekerdt, J.-M. Jehng, F.D. Hardcastle, I.E. Wachs, J. Phys. Chem. 95 (1991) 8791.
[33] L. Wang, W.K. Hall, J. Catal. 77 (1982) 232.
[34] R. López Cordero, A. López Agudo, Appl. Catal. A: Gen. 202 (2000) 23.
[35] L. Qu, W. Zhang, P.J. Kooyman, R. Prins, J. Catal. 215 (2003) 7.
[36] P. Betancourt, A. Rives, R. Hubaut, C.E. Scott, J. Goldwasser, Appl. Catal. A: Gen. 170 (1998) 307.
[37] A. Tanksale, J.N. Beltramini, J.A. Dumesic, G.Q. Lu, J. Catal. 258 (2008) 366.
[38] D.D. Whitehurst, T. Isoda, I. Mochida, Adv. Catal. 42 (1998) 345.